THE JOURNAL OF PHYSICAL CHEMISTRY Letters

Letter

pubs.acs.org/JPCL

Unusual Electronic Structure of the Donor–Acceptor Cocrystal Formed by Dithieno[3,2-*a*:2′,3′-*c*]phenazine and 7,7,8,8-Tetracyanoquinodimethane

Qianxiang Ai,[†] Yulia A. Getmanenko,*[,‡] Karol Jarolimek,[†] Raúl Castañeda,[‡] Tatiana V. Timofeeva,[‡] and Chad Risko*[,†]

[†]Department of Chemistry & Center for Applied Energy Research, University of Kentucky, Lexington, Kentucky 40506-0055, United States

[‡]Department of Chemistry, New Mexico Highlands University, Las Vegas, New Mexico 87701, United States

Supporting Information

ABSTRACT: Mixed cocrystals derived from electron-rich donor (D) and electron-deficient acceptor (A) molecules showcase electronic, optical, and magnetic properties of interest for a wide range of applications. We explore the structural and electronic properties of a cocrystal synthesized from dithieno-[3,2-*a*:2′,3′-*c*]phenazine (DTPhz) and 7,7,8,8-tetracyanoquinodimethane (TCNQ), which has a mixed-stack packing arrangement of the (π-electronic) face-to-face stacks in a 2:1 D:A stoichiometry. Density functional theory investigations reveal that the primary electronic characteristics of the cocrystal are not determined by electronic interactions along the face-to-face stacks, but rather they are characterized by stronger electronic interactions orthogonal to these stacks that follow the edge-to-edge donor–donor or acceptor–acceptor contacts. These distinctive electronic characteristics portend semiconducting properties that are unusual for semiconducting mixed cocrystals and suggest further potential to design organic semiconductors with orthogonal transport characteristics for different charge carriers.

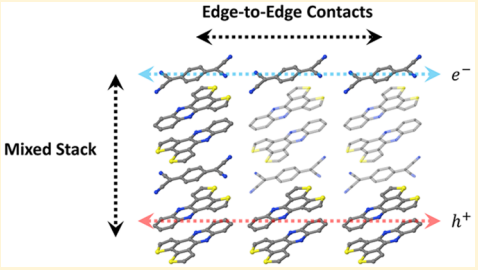

Organic electronic materials (OEMs) have held the interest of academic and industrial researchers for the last few decades due to the capability of the synthetic chemist to tailor material properties through molecular design. While the majority of OEMs are composed of a single molecular species, multicomponent molecular blends offer pathways to create materials with distinctive electrical, optical, or magnetic response that are difficult to achieve otherwise. OEM derived from charge-transfer complexes[1,2] (formed when electron-rich donor (D) molecules are mixed with electron-deficient acceptor (A) molecules), for instance, have demonstrated metallic conductivity,[3−5] superconductivity,[6−9] ambipolar semiconductor transport,[10−14] ferroelectric response,[15−17] and magnetoresistance;[18] moreover, materials derived from bilayers or blends of D and A molecules form the heart of organic solar cell technologies.[19−21] Of specific interest to this work are crystalline DA materials (DA cocrystals), where precise knowledge of the molecular spatial arrangement allows for direct interrogation of the relationships between molecular composition and architecture and material characteristics. DA cocrystals with 1:1 D:A stoichiometric ratios generally feature the D and A molecules packed in segregated- (i.e., a column of D molecules, ···D−D−D−D···, aligned next to a column of A molecules, ···A−A−A−A···) or mixed-stack (i.e., a column of D and A molecules stacked in a regular ···D−A−D−A··· pattern) arrangements.[1] Cocrystals formed by varying the D:A stoichiometric ratios, for example, 2:1 and 3:1, have also been created and studied,[22−25] as these blends offer more varied possibilities in terms of the molecular packing arrangements and materials properties. While some guidelines exist, there are limited a priori design principles that can be followed to predict the stoichiometry, stacking arrangements, or degree of charge-transfer character for a given set of D and A molecules, and there is no expectation as to how the molecular variables determine the material electronic, magnetic, or optical response.[23]

Recent theoretical efforts concerning the semiconductor behavior of mixed-stack cocrystals have revealed that the electronic properties can frequently be described through a superexchange (SE) mechanism.[12−14,22,26−28] Here, for instance, focusing on hole transport, holes transported along ···D−A−D−A··· mixed stacks move among the D sites through an electronic coupling that is mediated by the bridging A molecule; a like-wise D-mediated electronic coupling is required for electron transport among A sites. These SE electronic couplings, computed among D−A−D (or A−D−A) complexes extracted from DA cocrystals, correlate well with valence (conduction) band dispersions and hole (electron) effective masses determined through periodic electronic-structure calculations to provide a detailed description of the

Received: July 13, 2017
Accepted: September 1, 2017
Published: September 1, 2017

DOI: 10.1021/acs.jpclett.7b01816
J. Phys. Chem. Lett. 2017, 8, 4510−4515

material electronic characteristics; the same has been shown to be true for varied stoichiometric-induced stacking arrangements (e.g., ···A−D−D−A−D−D···).[22] In this contribution, we showcase an unusual situation where the SE mechanism does not describe the main transport characteristics of a mixed cocrystal, as the charge carriers of the valence and conduction bands are predicted to traverse perpendicular to the DA (mixed) stacking direction (i.e., not along the [π-electronic] face-to-face stacks). While previous reports have indicated somewhat strong SE and direct electronic couplings among molecules in neighboring mixed-stack columns and the possibility for 2D or 3D transport characteristics, these contacts have not been demonstrated to be the primary electronic interactions that determine the crystal electronic band structure.[22,29,30]

The DA cocrystal of interest in this study was synthesized by combining dithieno[3,2-*a*:2′,3′-*c*]phenazine (DTPhz) as the D moiety and 7,7,8,8-tetracyanoquinodimethane (TCNQ) as the A moiety (Figure 1). DTPhz has been exploited as an acceptor unit in DA copolymers employed in solar cells,[31,32] as a light absorber in dye-sensitized solar cells,[33] and as an anion probe.[34] TCNQ and its derivative forms are among the most widely used A units in the DA cocrystal literature.[1,4,8,12,22,23,25,29,35,36] Details of the synthesis and characterization of DTPhz are provided in the Supporting Information (SI); TCNQ was used as received. DTPhz−TCNQ cocrystals were formed by the slow evaporation of chloroform or, alternatively, acetonitrile from a solution containing an equimolar mixture of DTPhz and TCNQ. Several dark-colored cocrystals (see Figure S8 in the SI) were detected by microscopy as a minor component surrounded by the respective single-component crystals of DTPhz and TCNQ.

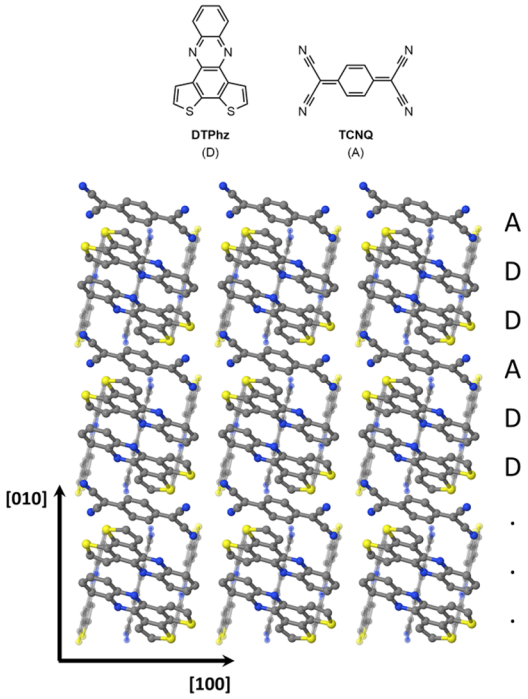

Figure 1. Chemical structures of DTPhz (dithieno[3,2-*a*:2′,3′-*c*]phenazine) and TCNQ (7,7,8,8-tetracyanoquinodimethane) and their crystalline packing arrangement. Two layers stacked along the [001] direction are shown. The [010] and [100] directions are depicted. For convenience, the ··· A−D−D··· packing repeat is also identified. Views along different projection planes are provided in the Supporting Information (SI, Figure S9).

The DTPhz−TCNQ cocrystal structure (Cambridge Structural Database (CSD) Reference Number 1561865), identified by single-crystal X-ray diffraction at a temperature of 100 K, is triclinic within the $P\bar{1}$ space group; see Table S1 for a listing of crystallographic data. DTPhz (D) and TCNQ (A) form a mixed-stack, face-to-face packing motif that follows a ···A−D−D−A−D−D··· (1:2 A:D ratio) pattern. The molecular packing arrangements in the DTPhz−TCNQ cocrystal can be described as an alternating layered structure. The layers are perpendicular to the *c*-axis and are occupied by mixed ···A−D−D··· stacks oriented in either the [010] direction in one layer or the [100] direction in the next layer. Importantly, these noncollinear stacks have different periodicities and therefore cannot be related by symmetry operations. Further details regarding the layer geometries are provided in Figure S9 and Table S2. Throughout the remainder of this report, we will refer to these layers as the "α layer" (i.e., the mixed stacks that are oriented in the [010] direction) or the "β layer" (i.e., the mixed stacks that are oriented in the [100] direction).

Because the main charge-carrier transport mechanism in semiconducting DA cocrystals is generally considered to invoke the SE mechanism along the mixed-stack packing direction, we begin the description of the electronic characteristics of the DTPhz−TCNQ cocrystal in this framework. The SE electronic couplings are evaluated by the so-called energy-splitting approach (t^{ES})[13] at the PBE/6-31G(d,p) level of theory,[37−39] making use of the occupied energy levels of the neutral D−A−D triad for holes and the unoccupied energy levels of the neutral A−D−D−A tetrad for electrons (in the geometries from the experimental crystal structure), through

$$t^{ES} = \frac{E_{H(L+1)} - E_{H-1(L)}}{2} \quad (1)$$

where $E_{H(L+1)}$ and $E_{H-1(L)}$ are the energies of the HOMO (LUMO+1) and HOMO−1 (LUMO), respectively. For both the D−A−D triad and A−D−D−A tetrad, t^{ES} is very small at 7 and 2 meV, respectively, for the α layer and 16 and 8 meV, respectively, for the β layer; t^{ES} determined at the PBE0/6-31G(d,p) level of theory shows very similar trends (Table S8), as expected.[40] These very small t^{ES} suggest that if the DTPhz−TCNQ cocrystals were to be considered for semiconducting applications then charge-carrier transport through the ··· A−D−D−A−D−D··· mixed-stacks would be limited.

This hypothesis is reinforced through analysis of the DTPhz−TCNQ cocrystal electronic band structure (Figure 2) and band-decomposed charge densities (Figure 3), computed at the PBE level of theory with the projector augmented-wave method.[38,41−43] Note that all results reported here are for calculations that are carried out on the experimental molecular and crystal structures; full details of the calculations for the results described here and calculations and results where the density functional incorporates varying amounts of exact exchange or dispersion corrections are used in the relaxation of the unit cell and molecular structures are provided in the SI. Strictly, the DTPhz−TCNQ cocrystal is an indirect semiconductor with its valence band maximum (VBM) at the Z point and conduction band minimum (CBM) at the Γ point, although the indirect gap is nearly indistinguishable from the smallest direct gap found at the Γ point; definitions of the high-symmetry points in the first Brillouin zone, following the scheme proposed by Setyawan and Curtarolo,[44] are available in

DOI: 10.1021/acs.jpclett.7b01816
J. Phys. Chem. Lett. 2017, 8, 4510−4515

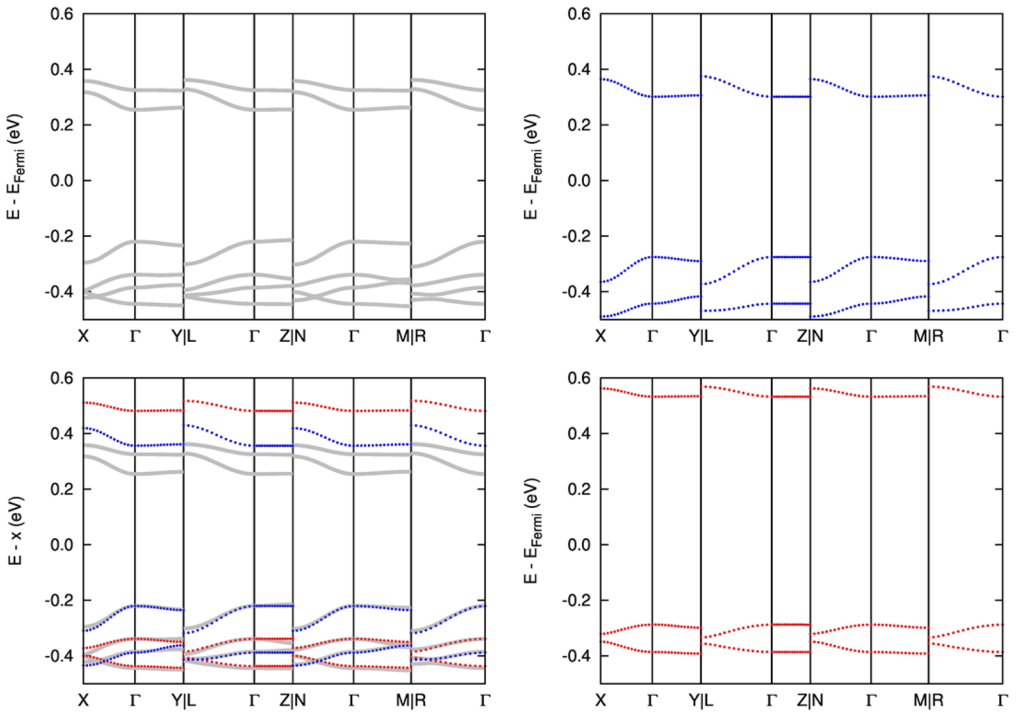

Figure 2. Electronic band structures of the DTPhz−TCNQ cocrystal (top left), α layer (top right), and β layer (bottom right). A superposition of the α layer and β layer band structures overlaid on top of the cocrystal band structure (bottom left); here the α layer and β layer band structures are shifted so that their VBM match the VBM and VB-1M of the cocrystal, respectively, with the amount of the shift represented by the variable x.

the SI. For both the valence and conduction bands, the largest bandwidth is found along the $R \rightarrow \Gamma$ direction, while the largest curvature is found at Γ along the $\Gamma \rightarrow X$ direction, which coincides with the [100] direction. The smallest effective mass (m^*) for holes is determined[45] to be $1.53m_0$, while that for electrons is $1.80m_0$ (m_0 is the rest mass of electron); the corresponding principal axes of the effective mass tensors point along the [100] direction. The valence and conduction band charge densities, interestingly, only reside on molecules in the α layer, that is, there is no charge density in the β layer. Furthermore, the charge densities are highly localized within the mixed stacks: The valence band charge density resides on the D−D stack, while the conduction band charge density is localized solely on A. The lack of charge density distribution among the D and A units along the mixed-stack direction is consistent with the small t^{ES}. Furthermore, determination of the direct electronic coupling computed by the fragment-orbital approach, t^{FO},[46−48] between the D (HOMO) and A (LUMO) is small at t^{FO} = 6 meV. Analysis of the TCNQ bond lengths in the DTPhz−TCNQ cocrystal shows negligible difference when compared with TCNQ in pure crystals. Both of these results suggest very little charge transfer[22] between the D and A components in the DTPhz−TCNQ cocrystal. Interestingly, the inspection of the valence and conduction band charge densities indicates that within the α layer there is extended electronic communication between mixed stacks that follow edge-to-edge interactions among D (valence band) or A (conduction band) molecules, respectively. We note that the incorporation of large amounts of exact exchange in the PBE functional or the relaxation of the molecules and unit cells with dispersion-corrected PBE (and PBE0) does not change the analysis of the electronic band structure; see the SI for further details.[49]

Electronic band structures of isolated α and β layers, with periodicity identical to that of the cocrystal (Figure 2), were determined to investigate the electronic characteristics in further detail. Superposition of the isolated layer band structures nearly returns that of the full cocrystal; the modest exception is a larger electronic band gap, which is due to the absence of dielectric screening between isolated layers.[50] This result implies small electronic interactions between the α layers and β layers, confirming that the separation of the layers is a valid approach. Furthermore, on the basis of the position and similarities of the band shapes, the α layer is suggested to be responsible for the valence and conduction bands in the DTPhz−TCNQ cocrystal. As noted above, however, the smallest effective masses for both holes and electrons in the cocrystal are found along the [100] direction, which appears to contradict the suggestion that the α layer is the active layer. However, considering the localization of the charge densities, it is possible that the electronic couplings within [010] stacks are weaker than those between [010] stacks along [100] direction. Indeed, the electronic couplings for edge-to-edge (interstack) donors (t^{ES} = 17 meV; t^{FO} = 17 meV) and acceptors (t^{ES} = 15 meV; t^{FO} = 15 meV) interactions along the [100] direction in the α layer are larger than those determined for the SE mechanism along the stacks; the intrastack DD electronic couplings are large (t^{ES} = 68 meV; t^{FO} = 64 meV), although these DD stacks are essentially isolated from each other in the mixed-stack packing direction because of a lack of electronic communication through the A moieties (see above). Notably, both methods used to evaluate the electronic couplings provide similar results and follow the expected $4t \approx W$ (where W is the width of the valence or conduction band) relationship for a 1D chain; this is consistent with the fact that there should be little-to-no variation in molecular polarization along a 1D stack.

To further validate this hypothesis, the experimental crystal structures were used to prepare unit cells that contain only donors or only acceptors in the α layer, that is, idealized,

DOI: 10.1021/acs.jpclett.7b01816
J. Phys. Chem. Lett. 2017, 8, 4510−4515

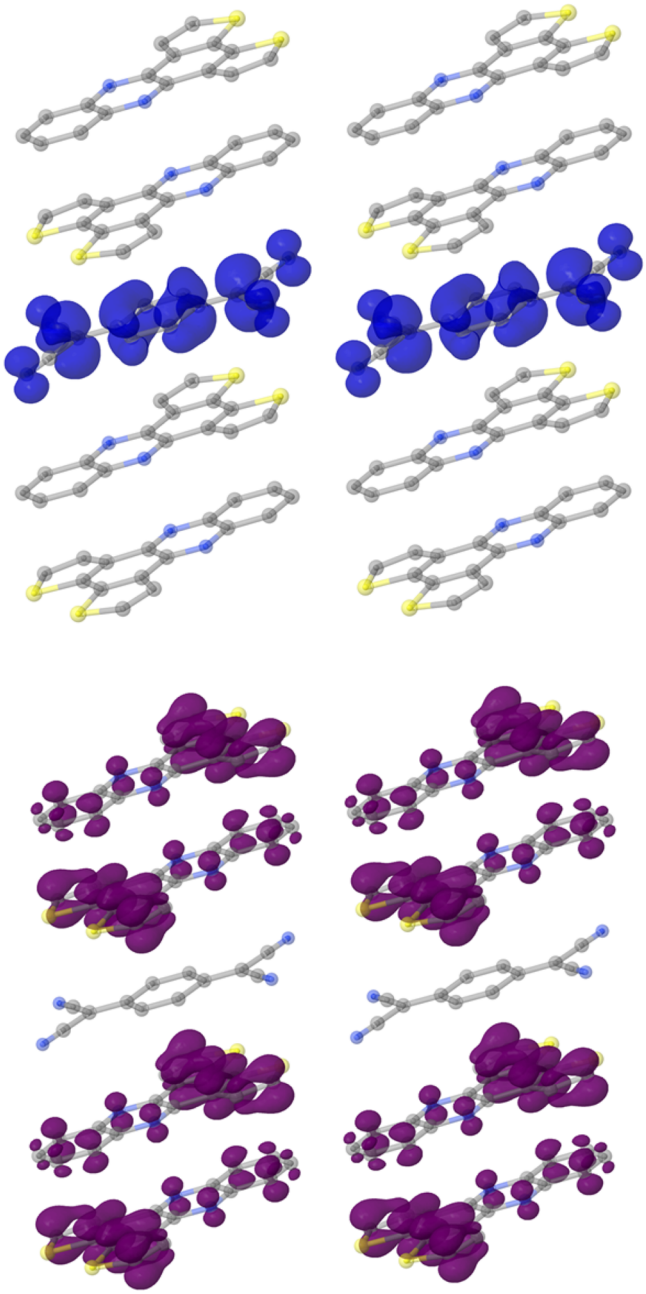

Figure 3. Band-decomposed charge densities of the conduction band (blue) (top) and valence band (purple) (bottom) for the DTPhz–TCNQ cocrystal α layer. The cutoff of charge density is set to 0.02 eÅ^{-3}.

segregated 1D edge-to-edge chains of donors or acceptors; note that the β layer is removed completely. The unit-cell parameters are kept the same as in the cocrystal. As with the previous decomposition of the cocrystal into layers, there is a noticeable similarity among the band structures of these model D and A chains and that of the full cocrystal, as demonstrated by the superposition of the three band structures in Figure 4.

From this analysis, we can conclude a rather distinctive electronic structure for the DTPhz–TCNQ cocrystal. Although the DTPhz and TCNQ molecules form mixed (π-electron) face-to-face stacks, the valence and conduction bands follow edge-to-edge contacts among donor molecules and acceptor molecules, respectively, between stacks. This is an unusual

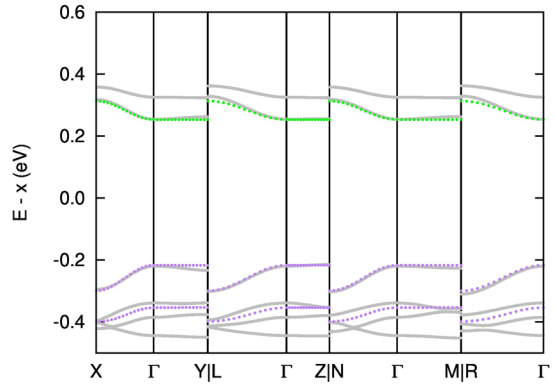

Figure 4. Superposed electronic band structures of the donor-only (DTPhz; purple) and acceptor-only (TCNQ; green) stacks in the α layer. The band structure of the full cocrystal (DTPhz–TCNQ; gray) is also shown. Note that the VBM of donor-only structure was shifted to that in the full DTPhz–TCNQ cocrystal band structure; the same is true for the CBM of acceptor-only structure. The amount of the shift is represented by the variable x.

behavior for materials with significant (π-electron) face-to-face stacking arrangements. Hence, one might expect the transport of holes and electrons to be orthogonal to the mixed face-to-face stacks, as shown schematically in Figure 5.

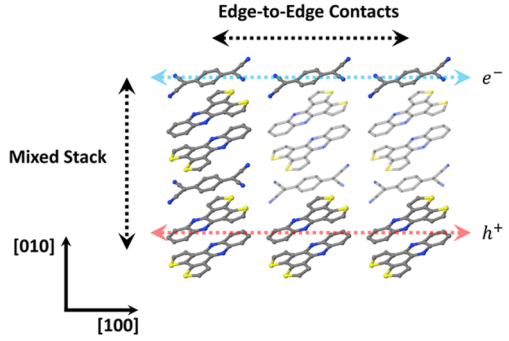

Figure 5. Proposed charge-carrier transport pathways in the DTPhz–TCNQ cocrystal.

The electronic characteristics of the DTPhz–TCNQ cocrystal, when combined with previous reports of potential 2D and 3D charge-carrier transport pathways in DA cocrystals,[22,29,30,51] offer distinctive paradigms for the development of mixed cocrystals with intriguing charge-carrier transport properties. For instance, one could envision materials where the transport of holes or electrons could be favored along the mixed-stack direction, while the alternate charge carrier would be favored along an orthogonal direction. Such multidirectional charge-carrier transport characteristics within a single material could lead to alternative device designs for advanced (opto)electronics applications. However, much work remains to be able to make material predictions based on the properties of isolated D and A constituents.

■ ASSOCIATED CONTENT

Supporting Information

The Supporting Information is available free of charge on the ACS Publications website at DOI: 10.1021/acs.jpclett.7b01816.

Molecular and cocrystal synthesis details; experimental characterization, including cyclic voltammetry and X-ray

DOI: 10.1021/acs.jpclett.7b01816
J. Phys. Chem. Lett. 2017, 8, 4510–4515

crystallography; details of the computational methods and additional DFT results. (PDF)

AUTHOR INFORMATION

Corresponding Authors

*C.R.: E-mail: chad.risko@uky.edu,
*Y.A.G.: E-mail: yu_getmanenko@yahoo.com.

ORCID

Yulia A. Getmanenko: 0000-0003-4099-8517
Tatiana V. Timofeeva: 0000-0001-7475-3206
Chad Risko: 0000-0001-9838-5233

Notes

The authors declare no competing financial interest.

ACKNOWLEDGMENTS

The work at the University of Kentucky was supported in part by the National Science Foundation (NSF DMR-1627428) and start-up funds provided by the University of Kentucky Vice President for Research. The work at New Mexico Highlands University was supported in part by the NSF via DMR-0934212, DMR-1523611 (PREM), and IIA-130134, with additional support from the Center for Emergent Materials, an NSF MRSEC under award number DMR-1420451, and New Mexico EPSCoR Infrastructure Seed Award. Supercomputing resources on the Lipscomb High Performance Computing Cluster were provided by the University of Kentucky Information Technology Department and Center for Computational Sciences (CCS). We thank Dr. Sean Ryno for helpful discussions and Dr. Boris B. Averkiev for help with X-ray structural analysis. Y.A.G. thanks Professor Seth R. Marder for providing access to the electrochemical setup, synthetic facility, and reagents for the preparation of some of the TMS-BDDO starting material and Professor Yang Qin for providing access to synthetic and NMR facilities.

REFERENCES

(1) Goetz, K. P.; Vermeulen, D.; Payne, M. E.; Kloc, C.; McNeil, L. E.; Jurchescu, O. D. Charge-transfer complexes: new perspectives on an old class of compounds. *J. Mater. Chem. C* **2014**, *2* (17), 3065−3076.

(2) Zhang, J.; Xu, W.; Sheng, P.; Zhao, G.; Zhu, D. Organic Donor−Acceptor Complexes as Novel Organic Semiconductors. *Acc. Chem. Res.* **2017**, *50*, 1654.

(3) Ferraris, J.; Cowan, D. O.; Walatka, V.; Perlstein, J. H. Electron transfer in a new highly conducting donor-acceptor complex. *J. Am. Chem. Soc.* **1973**, *95* (3), 948−949.

(4) Torrance, J. B. The difference between metallic and insulating salts of tetracyanoquinodimethone (TCNQ): how to design an organic metal. *Acc. Chem. Res.* **1979**, *12* (3), 79−86.

(5) Torrance, J. B. An Overview of Organic Charge-Transfer Solids: Insulators, Metals, and the Neutral-Ionic Transition. *Mol. Cryst. Liq. Cryst.* **1985**, *126* (1), 55−67.

(6) Saito, G.; Yoshida, Y. Development of Conductive Organic Molecular Assemblies: Organic Metals, Superconductors, and Exotic Functional Materials. *Bull. Chem. Soc. Jpn.* **2007**, *80* (1), 1−137.

(7) Jerome, D.; Mazaud, A.; Ribault, M.; Bechgaard, K. Superconductivity in a synthetic organic conductor (TMTSF)2PF6. *J. Phys., Lett.* **1980**, *41*, 95−98.

(8) Jérome, D. Organic Conductors: From Charge Density Wave TTF−TCNQ to Superconducting (TMTSF)2PF6. *Chem. Rev.* **2004**, *104* (11), 5565−5592.

(9) Mori, T.; Kawamoto, T. Organic conductors-from fundamentals to nonlinear conductivity. *Annu. Rep. Prog. Chem., Sect. C: Phys. Chem.* **2007**, *103* (0), 134−172.

(10) Chen, X.; Zhang, G.; Luo, H.; Li, Y.; Liu, Z.; Zhang, D. Ambipolar charge-transport property for the D-A complex with naphthalene diimide motif. *J. Mater. Chem. C* **2014**, *2* (16), 2869−2876.

(11) Park, S. K.; Varghese, S.; Kim, J. H.; Yoon, S.-J.; Kwon, O. K.; An, B.-K.; Gierschner, J.; Park, S. Y. Tailor-Made Highly Luminescent and Ambipolar Transporting Organic Mixed Stacked Charge-Transfer Crystals: An Isometric Donor−Acceptor Approach. *J. Am. Chem. Soc.* **2013**, *135* (12), 4757−4764.

(12) Zhang, J.; Geng, H.; Virk, T. S.; Zhao, Y.; Tan, J.; Di, C.-a.; Xu, W.; Singh, K.; Hu, W.; Shuai, Z.; Liu, Y.; Zhu, D. Sulfur-Bridged Annulene-TCNQ Co-Crystal: A Self-Assembled "Molecular Level Heterojunction" with Air Stable Ambipolar Charge Transport Behavior. *Adv. Mater.* **2012**, *24* (19), 2603−2607.

(13) Zhu, L.; Yi, Y.; Li, Y.; Kim, E.-G.; Coropceanu, V.; Brédas, J.-L. Prediction of Remarkable Ambipolar Charge-Transport Characteristics in Organic Mixed-Stack Charge-Transfer Crystals. *J. Am. Chem. Soc.* **2012**, *134* (4), 2340−2347.

(14) Qin, Y.; Cheng, C.; Geng, H.; Wang, C.; Hu, W.; Xu, W.; Shuai, Z.; Zhu, D. Efficient ambipolar transport properties in alternate stacking donor-acceptor complexes: from experiment to theory. *Phys. Chem. Chem. Phys.* **2016**, *18* (20), 14094−14103.

(15) Kagawa, F.; Horiuchi, S.; Tokunaga, M.; Fujioka, J.; Tokura, Y. Ferroelectricity in a one-dimensional organic quantum magnet. *Nat. Phys.* **2010**, *6* (3), 169−172.

(16) Kobayashi, K.; Horiuchi, S.; Kumai, R.; Kagawa, F.; Murakami, Y.; Tokura, Y. Electronic Ferroelectricity in a Molecular Crystal with Large Polarization Directing Antiparallel to Ionic Displacement. *Phys. Rev. Lett.* **2012**, *108* (23), 237601.

(17) Cheng, L.; Crumlin, E. J.; Chen, W.; Qiao, R. M.; Hou, H. M.; Lux, S. F.; Zorba, V.; Russo, R.; Kostecki, R.; Liu, Z.; Persson, K.; Yang, W. L.; Cabana, J.; Richardson, T.; Chen, G. Y.; Doeff, M. The origin of high electrolyte-electrode interfacial resistances in lithium cells containing garnet type solid electrolytes. *Phys. Chem. Chem. Phys.* **2014**, *16* (34), 18294−18300.

(18) Lee, T.-H.; Li, J.-H.; Huang, W.-S.; Hu, B.; Huang, J. C. A.; Guo, T.-F.; Wen, T.-C. Magnetoconductance responses in organic charge-transfer-complex molecules. *Appl. Phys. Lett.* **2011**, *99* (7), 073307.

(19) Tang, C. W. Two layer organic photovoltaic cell. *Appl. Phys. Lett.* **1986**, *48* (2), 183−185.

(20) Halls, J. J. M.; Walsh, C. A.; Greenham, N. C.; Marseglia, E. A.; Friend, R. H.; Moratti, S. C.; Holmes, A. B. Efficient photodiodes from interpenetrating polymer networks. *Nature* **1995**, *376* (6540), 498−500.

(21) Yu, G.; Gao, J.; Hummelen, J. C.; Wudl, F.; Heeger, A. J. Polymer Photovoltaic Cells: Enhanced Efficiencies via a Network of Internal Donor-Acceptor Heterojunctions. *Science* **1995**, *270* (5243), 1789−1791.

(22) Vermeulen, D.; Zhu, L. Y.; Goetz, K. P.; Hu, P.; Jiang, H.; Day, C. S.; Jurchescu, O. D.; Coropceanu, V.; Kloc, C.; McNeil, L. E. Charge Transport Properties of Perylene−TCNQ Crystals: The Effect of Stoichiometry. *J. Phys. Chem. C* **2014**, *118* (42), 24688−24696.

(23) Hu, P.; Du, K.; Wei, F.; Jiang, H.; Kloc, C. Crystal Growth, HOMO−LUMO Engineering, and Charge Transfer Degree in Perylene-FxTCNQ (x = 1, 2, 4) Organic Charge Transfer Binary Compounds. *Cryst. Growth Des.* **2016**, *16* (5), 3019−3027.

(24) Kataeva, O.; Khrizanforov, M.; Budnikova, Y.; Islamov, D.; Burganov, T.; Vandyukov, A.; Lyssenko, K.; Mahns, B.; Nohr, M.; Hampel, S.; Knupfer, M. Crystal Growth, Dynamic and Charge Transfer Properties of New Coronene Charge Transfer Complexes. *Cryst. Growth Des.* **2016**, *16* (1), 331−338.

(25) Salzillo, T.; Masino, M.; Kociok-Köhn, G.; Di Nuzzo, D.; Venuti, E.; Della Valle, R. G.; Vanossi, D.; Fontanesi, C.; Girlando, A.; Brillante, A.; Da Como, E. Structure, Stoichiometry, and Charge Transfer in Cocrystals of Perylene with TCNQ-Fx. *Cryst. Growth Des.* **2016**, *16* (5), 3028−3036.

(26) Fonari, A.; Sutton, C.; Brédas, J.-L.; Coropceanu, V. Impact of exact exchange in the description of the electronic structure of organic

DOI: 10.1021/acs.jpclett.7b01816
J. Phys. Chem. Lett. 2017, 8, 4510−4515

charge-transfer molecular crystals. *Phys. Rev. B: Condens. Matter Mater. Phys.* **2014**, *90* (16), 165205.
(27) Fonari, A.; Corbin, N. S.; Vermeulen, D.; Goetz, K. P.; Jurchescu, O. D.; McNeil, L. E.; Bredas, J. L.; Coropceanu, V. Vibrational properties of organic donor-acceptor molecular crystals: Anthracene-pyromellitic-dianhydride (PMDA) as a case study. *J. Chem. Phys.* **2015**, *143* (22), 224503.
(28) Geng, H.; Zheng, X.; Shuai, Z.; Zhu, L.; Yi, Y. Understanding the Charge Transport and Polarities in Organic Donor−Acceptor Mixed-Stack Crystals: Molecular Insights from the Super-Exchange Couplings. *Adv. Mater.* **2015**, *27* (8), 1443−1449.
(29) Zhang, J.; Liu, G.; Zhou, Y.; Long, G.; Gu, P.; Zhang, Q. Solvent Accommodation: Functionalities Can Be Tailored Through Co-Crystallization Based on 1:1 Coronene-F4TCNQ Charge-Transfer Complex. *ACS Appl. Mater. Interfaces* **2017**, *9* (2), 1183−1188.
(30) Zhu, L.; Yi, Y.; Fonari, A.; Corbin, N. S.; Coropceanu, V.; Brédas, J.-L. Electronic Properties of Mixed-Stack Organic Charge-Transfer Crystals. *J. Phys. Chem. C* **2014**, *118* (26), 14150−14156.
(31) Fan, J. Z.; Zhang, Y.; Lang, C. L.; Qiu, M.; Song, J. S.; Yang, R. Q.; Guo, F. Y.; Yu, Q. J.; Wang, J. Z.; Zhao, L. C. Side chain effect on poly(beznodithiophene-co-dithienobenzoquinoxaline) and their applications for polymer solar cells. *Polymer* **2016**, *82*, 228−237.
(32) Zhang, Y.; Zou, J. Y.; Yip, H. L.; Chen, K. S.; Davies, J. A.; Sun, Y.; Jen, A. K. Y. Synthesis, Characterization, Charge Transport, and Photovoltaic Properties of Dithienobenzoquinoxaline- and Dithienobenzopyridopyrazine-Based Conjugated Polymers. *Macromolecules* **2011**, *44* (12), 4752−4758.
(33) Richard, C. A.; Pan, Z. X.; Hsu, H. Y.; Cekli, S.; Schanze, K. S.; Reynolds, J. R. Effect of Isomerism and Chain Length on Electronic Structure, Photophysics, and Sensitizer Efficiency in Quadrupolar (Donor)(2)-Acceptor Systems for Application in Dye-Sensitized Solar Cells. *ACS Appl. Mater. Interfaces* **2014**, *6* (7), 5221−5227.
(34) El-Assaad, T. H.; Shiring, S. B.; Getmanenko, Y. A.; Hallal, K. M.; Bredas, J. L.; Marder, S. R.; Al-Sayah, M. H.; Kaafarani, B. R. Dithieno[3,2-*a*:2′,3′-*c*]phenazine-based chemical probe for anions: a spectroscopic study of binding. *RSC Adv.* **2015**, *5* (54), 43303−43311.
(35) Rudloff, M.; Ackermann, K.; Huth, M.; Jeschke, H. O.; Tomic, M.; Valenti, R.; Wolfram, B.; Broring, M.; Bolte, M.; Chercka, D.; Baumgarten, M.; Mullen, K. Charge transfer tuning by chemical substitution and uniaxial pressure in the organic complex tetramethoxypyrene-tetracyanoquinodimethane. *Phys. Chem. Chem. Phys.* **2015**, *17* (6), 4118−4126.
(36) Zhu, L.; Geng, H.; Yi, Y.; Wei, Z. Charge transport in organic donor-acceptor mixed-stack crystals: the role of nonlocal electron-phonon couplings. *Phys. Chem. Chem. Phys.* **2017**, *19* (6), 4418−4425.
(37) Frisch, M. J.; Trucks, G. W.; Schlegel, H. B.; Scuseria, G. E.; Robb, M. A.; Cheeseman, J. R.; Scalmani, G.; Barone, V.; Mennucci, B.; Petersson, G. A.; Nakatsuji, H.; Caricato, M.; Li, X.; Hratchian, H. P.; Izmaylov, A. F.; Bloino, J.; Zheng, G.; Sonnenberg, J. L.; Hada, M.; Ehara, M.; Toyota, K.; Fukuda, R.; Hasegawa, J.; Ishida, M.; Nakajima, T.; Honda, Y.; Kitao, O.; Nakai, H.; Vreven, T.; Montgomery, J. A.; Peralta, J. E.; Ogliaro, F.; Bearpark, M.; Heyd, J. J.; Brothers, E.; Kudin, K. N.; Staroverov, V. N.; Kobayashi, R.; Normand, J.; Raghavachari, K.; Rendell, A.; Burant, J. C.; Iyengar, S. S.; Tomasi, J.; Cossi, M.; Rega, N.; Millam, J. M.; Klene, M.; Knox, J. E.; Cross, J. B.; Bakken, V.; Adamo, C.; Jaramillo, J.; Gomperts, R.; Stratmann, R. E.; Yazyev, O.; Austin, A. J.; Cammi, R.; Pomelli, C.; Ochterski, J. W.; Martin, R. L.; Morokuma, K.; Zakrzewski, V. G.; Voth, G. A.; Salvador, P.; Dannenberg, J. J.; Dapprich, S.; Daniels, A. D.; Farkas; Foresman, J. B.; Ortiz, J. V.; Cioslowski, J.; Fox, D. J. *Gaussian 09*, Revision E.01; Gaussian, Inc.: Wallingford, CT, 2009.
(38) Perdew, J. P.; Chevary, J. A.; Vosko, S. H.; Jackson, K. A.; Pederson, M. R.; Singh, D. J.; Fiolhais, C. Atoms, molecules, solids, and surfaces: Applications of the generalized gradient approximation for exchange and correlation. *Phys. Rev. B: Condens. Matter Mater. Phys.* **1992**, *46* (11), 6671−6687.
(39) Hehre, W. J.; Ditchfield, R.; Pople, J. A. Self-consistent molecular orbital methods. XII. Further extensions of Gaussian—type basis sets for use in molecular orbital studies of organic molecules. *J. Chem. Phys.* **1972**, *56* (5), 2257−2261.
(40) Sutton, C.; Sears, J. S.; Coropceanu, V.; Brédas, J.-L. Understanding the Density Functional Dependence of DFT-Calculated Electronic Couplings in Organic Semiconductors. *J. Phys. Chem. Lett.* **2013**, *4* (6), 919−924.
(41) Blöchl, P. E. Projector augmented-wave method. *Phys. Rev. B: Condens. Matter Mater. Phys.* **1994**, *50* (24), 17953.
(42) Kresse, G.; Furthmüller, J. Efficiency of ab-initio total energy calculations for metals and semiconductors using a plane-wave basis set. *Comput. Mater. Sci.* **1996**, *6* (1), 15−50.
(43) Kresse, G.; Joubert, D. From ultrasoft pseudopotentials to the projector augmented-wave method. *Phys. Rev. B: Condens. Matter Mater. Phys.* **1999**, *59* (3), 1758−1775.
(44) Setyawan, W.; Curtarolo, S. High-throughput electronic band structure calculations: Challenges and tools. *Comput. Mater. Sci.* **2010**, *49* (2), 299−312.
(45) Fonari, A.; Sutton, C. *Effective Mass Calculator*, 2012.
(46) Valeev, E. F.; Coropceanu, V.; da Silva Filho, D. A.; Salman, S.; Brédas, J.-L. Effect of Electronic Polarization on Charge-Transport Parameters in Molecular Organic Semiconductors. *J. Am. Chem. Soc.* **2006**, *128* (30), 9882−9886.
(47) Coropceanu, V.; Cornil, J.; da Silva Filho, D. A.; Olivier, Y.; Silbey, R.; Brédas, J.-L. Charge Transport in Organic Semiconductors. *Chem. Rev.* **2007**, *107* (4), 926−952.
(48) Ryno, S. M. *Transfer Integral Calculator*, 2017.
(49) Steinmann, S. N.; Piemontesi, C.; Delachat, A.; Corminboeuf, C. Why are the Interaction Energies of Charge-Transfer Complexes Challenging for DFT? *J. Chem. Theory Comput.* **2012**, *8* (5), 1629−1640.
(50) Winther, K. T.; Thygesen, K. S. Band structure engineering in van der Waals heterostructures via dielectric screening: the GΔW method. *2D Mater.* **2017**, *4* (2), 025059.
(51) Miller, N. C.; Cho, E.; Junk, M. J. N.; Gysel, R.; Risko, C.; Kim, D.; Sweetnam, S.; Miller, C. E.; Richter, L. J.; Kline, R. J.; Heeney, M.; McCulloch, I.; Amassian, A.; Acevedo-Feliz, D.; Knox, C.; Hansen, M. R.; Dudenko, D.; Chmelka, B. F.; Toney, M. F.; Brédas, J.-L.; McGehee, M. D. Use of X-Ray Diffraction, Molecular Simulations, and Spectroscopy to Determine the Molecular Packing in a Polymer-Fullerene Bimolecular Crystal. *Adv. Mater.* **2012**, *24* (45), 6071−6079.

DOI: 10.1021/acs.jpclett.7b01816
J. Phys. Chem. Lett. 2017, 8, 4510−4515